JOURNAL OF AIRCRAFT
Vol. 46, No. 5, September–October 2009

Theoretical Predictions of F-16 Fighter Limit Cycle Oscillations for Flight Flutter Testing

Earl H. Dowell,* Jeffrey P. Thomas,† and Kenneth C. Hall‡
Duke University, Durham, North Carolina 27708-0300
and
Charles M. Denegri Jr.§
U.S. Air Force SEEK EAGLE Office, Eglin Air Force Base, Florida 32542-6865

DOI: 10.2514/1.42352

A computational investigation of the flutter onset and limit cycle oscillation behavior of various F-16 fighter weapons and stores configurations is presented. A nonlinear harmonic balance compressible Reynolds-averaged Navier–Stokes computational fluid dynamic flow solver is used to model the unsteady aerodynamics of the F-16 wing. Slender body/wing theory is used as an approximate method for accounting for the unsteady aerodynamic effects of wing-tip launchers and missiles. Details of the computational model are presented along with an examination of the sensitivity of computed aeroelastic behavior to characteristics and parameters of the structural and fluid dynamic model. Comparisons with flight-test data are also shown.

I. Introduction

THE SEEK EAGLE Office at Eglin Air Force Base performs an essential task in clearing new aircraft/stores configurations through flight tests for safe and effective operation. Many of these flight tests are for the F-16 aircraft which continues to be a workhorse for the U.S. Air Force with continually new stores (missiles, bombs, and fuel tanks) being considered for aircraft operations. Similar aeroelastic flight tests are expected for future fighter aircraft as they go into service in the coming years.

The number of needed flight tests is projected to be well beyond the financial and staff resources available. Hence there is a pressing need to identify the most critical aircraft/store configurations for the limited flight-test resources available and also insofar as possibly reduce the number of flight tests needed.

Virtual flight testing may be the answer. Using new improved computational capability that provides much more rapid solutions, computational simulation can help identify the most critical aircraft/store configuration and also has the potential of reducing the number of needed flight tests if confidence can be established in the capability of simulations to correlate with flight-test data.

A new methodology has been developed to produce these computer simulations based upon the notion that because the response is periodic in time, the solution need only be obtained over a single period of oscillation in time. By avoiding the traditional time marching solution which computes the long transient before a steady-state periodic oscillation is reached, computational times are reduced by a factor of 10–100. This enables a sufficiently rapid solution to make such simulations a practical reality for the flight-test engineer and support team. Future developments of this methodology hold the promise of further substantial reductions in computational cost and are being vigorously pursued. Also further refinements in the physical fidelity of the simulation models are being considered.

This paper is a summary of the research efforts reported by Thomas et al. in [1–4], where the harmonic balance (HB) technique for modeling nonlinear unsteady aerodynamics (see Hall et al. [5] and Thomas et al. [6–8]) is used to determine the limit cycle oscillation (LCO) behavior of the F-16 fighter aircraft.

Many other researchers are also actively modeling the aeroelastic behavior of the F-16 fighter; for example, Denegri and Dubben [9–11] are using doublet-lattice methods for flutter onset analysis and transonic small-disturbance methods for flutter onset and limit cycle oscillation prediction. Parker et al. [12,13] are using time-domain computational fluid dynamics (CFD) simulations to study the effects of viscosity in addition to modeling external stores for computed F-16 limit cycle oscillations. Lieu and Farhat [14] and Lieu et al. [15] are developing reduced order models for F-16 flutter analysis based upon proper orthogonal decomposition (POD). Prananta et al. [16] are using a time-domain coupled computational fluid dynamic and modal based structural method for modeling the limit cycle oscillation response of the F-16. Melville [17] has also recently investigated time-domain CFD simulations for modeling LCO response of the F-16.

Flutter onset and LCO response behavior of the F-16 fighter are in general dependent on the specific external stores being carried by the airplane as well as the Mach number and altitude at which the aircraft is being flown. In the following, we will demonstrate how a novel nonlinear frequency domain harmonic technique can be used to rapidly determine the flutter onset Mach number for a specified altitude and also the subsequent finite amplitude LCO dynamic response of the aircraft for higher Mach numbers beyond the flutter onset boundary.

The aerodynamic solver portion of the aeroelastic model consists of a high fidelity nonlinear unsteady frequency domain compressible Reynolds averaged Navier–Stokes (RANS) solver for the F-16 wing aerodynamic pressures. The structural portion consists of a linear modal based model using mode shapes and modal masses obtained from a NASTRAN finite element model of the entire airplane configuration including fuselage, horizontal tail, and external weapons and stores. The structural damping is taken to be zero in the present study, although recent investigations have studied the effect of this parameter as well.

Presented as Paper 1640 at the U.S. Air Force T&E Days, Destin, FL, 13–15 February 2007; received 24 November 2008; revision received 5 May 2009; accepted for publication 13 May 2009.

*William Holland Hall Professor, Department of Mechanical Engineering and Materials Science. Honorary Fellow AIAA.

†Research Assistant Professor, Department of Mechanical Engineering and Materials Science. Senior Member AIAA.

‡Julian Francis Abele Professor, Department of Mechanical Engineering and Materials Science. Associate Fellow AIAA.

§Principal Technical Advisor, Flutter Analysis and Test Methodology, 205 West D Avenue, Suite 348. Senior Member AIAA.

II. Computational Model

A. Structural Model

The structural portion of the aeroelastic model consists of modal masses and mode shapes obtained from a NASTRAN finite element model. Only antisymmetric modes are usually needed for wings with symmetrically placed stores because flutter onset and LCO are usually antisymmetric for the F-16, as has been previously demonstrated in flight-test experiments and computational studies by the present authors and others. Figure 1 shows the first two antisymmetric mode shapes of F-16 configuration 1. The mode shapes have been fit to the CFD grid using a sixth-order least-squares polynomial fitting technique.

Computations using both symmetric and antisymmetric structural modes have shown that the former may be omitted for wing-store combinations that have the same stores on each wing. However, for configurations that have different stores on each wing, both symmetric and antisymmetric modes must be retained.

Structural damping has also been investigated for a few configurations. It is found that for typical values of structural damping, the results do not change significantly.

B. Fluid Dynamic Model

Only the F-16 wing is modeled in the present CFD analysis. The effects of the fuselage, horizontal tail, vertical tail, external weapons, and stores as such are not modeled in the CFD solver. However, their structural inertia and stiffness are included in the structural part of the overall aeroelastic analysis. Later in the paper, slender body theory is used to account for the aerodynamic effects of the wing-tip launchers and missiles including fins. We have found the flutter onset Mach number to be very sensitive to the geometry of the F-16 wing tip. We currently do not have the capability in our CFD solver to model the detailed geometry of the wing-tip launcher and missiles. However, we have found the use of the aerodynamic slender body theory to model the wing-tip launchers and missiles to be an effective method.

The CFD method used in the present analysis is a variant of the standard Lax–Wendroff scheme [18–20] in conjunction with the one-equation turbulence model of Spalart and Allmaras [21]. As also reported in [1], Fig. 2 shows the computational grid for the F-16 wing surface (Fig. 2a) and wing symmetry plane (Fig. 2b). The mesh uses 65 (mesh i coordinate) computational nodes about the wing in the streamwise direction, 33 (mesh j coordinate) nodes

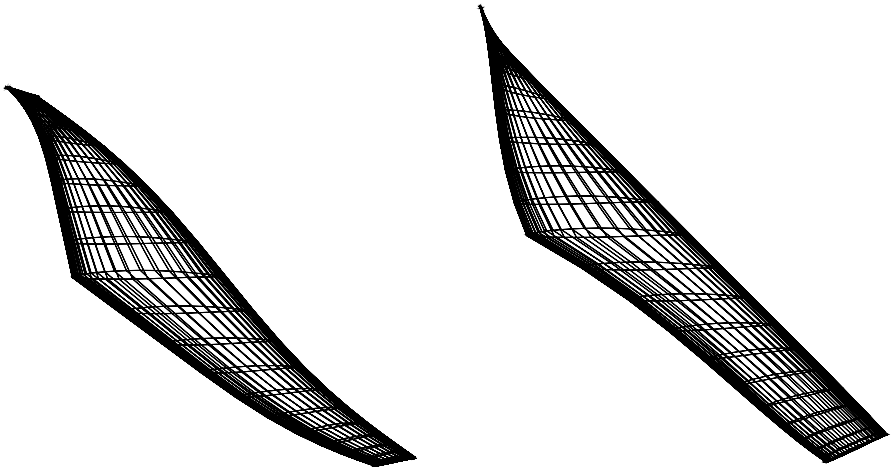

a) Mode 2 - 8.168 Hz **b) Mode 4 - 8.672 Hz**

Fig. 1 First two antisymmetric structural modes for F-16 configuration 1.

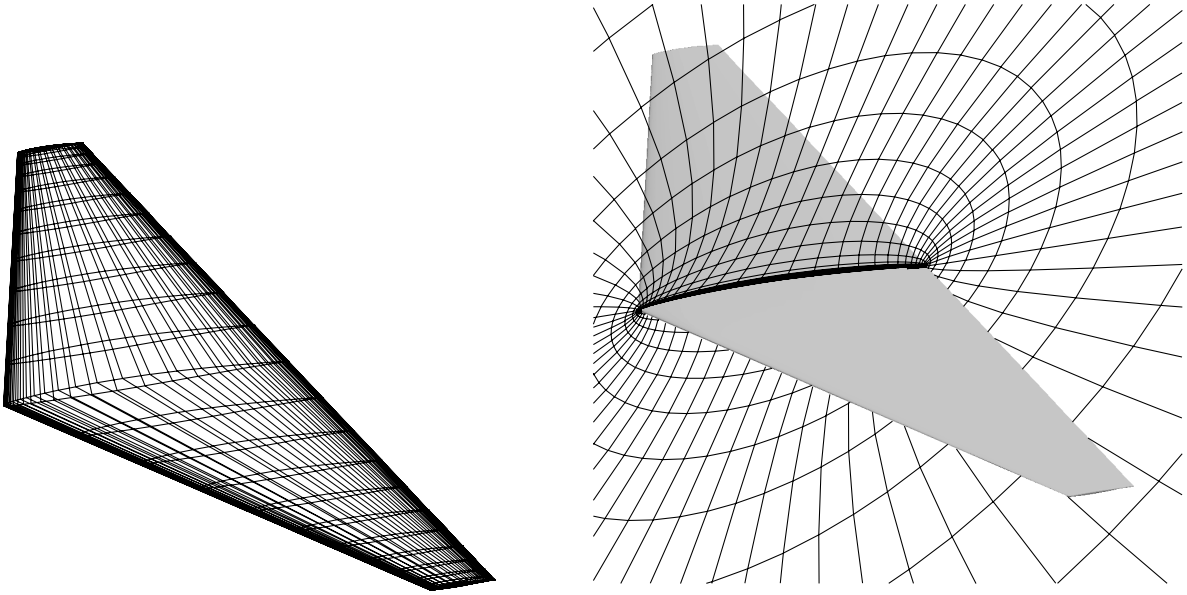

a) Wing surface grid **b) Wing symmetry plane grid**

Fig. 2 F-16 wing computational grid.

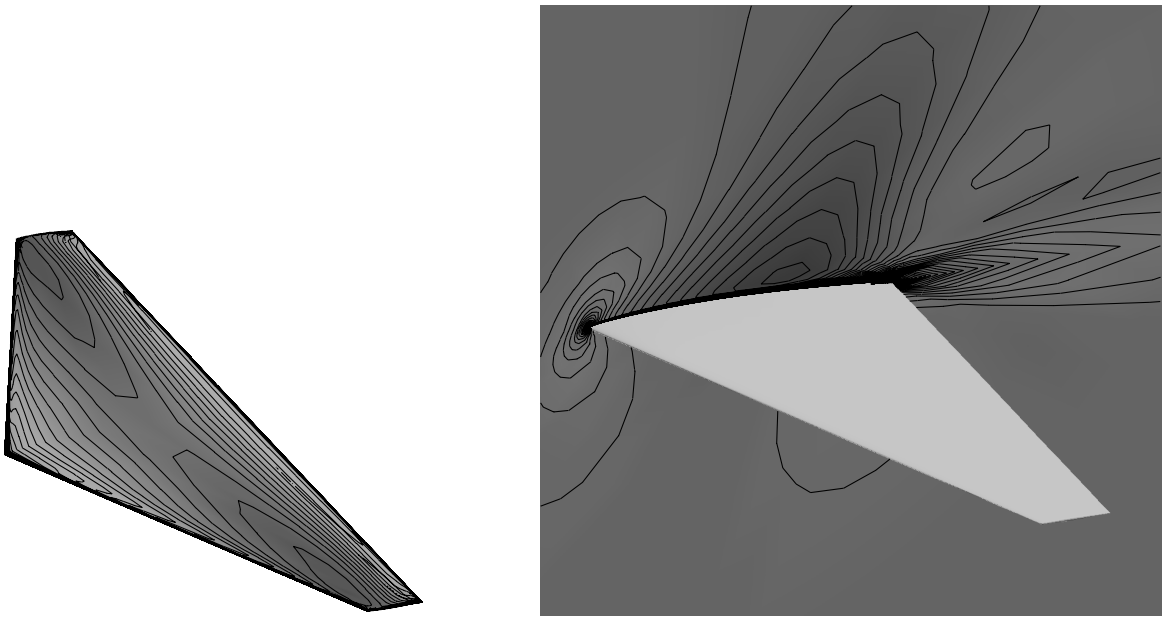

a) Surface pressure contours b) Wing symmetry mach number contours

Fig. 3 F-16 steady flow pressure and Mach number contours, $M_\infty = 0.9$, $\bar{\alpha}_0 = 1.5$ deg ., sea level altitude ($h = 0$ ft), $Re_{\infty_{c_r}} = 104 \times 10^6$.

normal to the wing, and 25 (mesh k coordinate) nodes along the span, with 12 more nodes wrapping around each wing tip for a total of 49 mesh points in the spanwise direction. The outer boundary of the grid extends 10 wing semispans from the midchord of the wing at the symmetry plane. Grid spacing near the surface is close enough to ensure that $y+$ distances (a measure boundary-layer grid resolution) are always less than 10 over the entire wing, and for most of the wing, less than five.

Figure 3 shows computed viscous steady flow surface pressure contours (Fig. 3a) and Mach number contours in the wing symmetry plane (Fig. 3b) for a freestream Mach number of $M_\infty = 0.9$, steady angle of attack of $\bar{\alpha}_0 = 1.5$ deg, and sea level altitude. Standard atmosphere conditions are assumed. For this Mach number and altitude, the Reynolds number based on the wing root chord is $Re_{\infty_{c_r}} = 104 \times 10^6$.

For the analysis presented in this paper, we consider straight and level flight, and as an initial approximation, we consider the angle of attack of $\bar{\alpha}_0 = 1.5$ deg to be constant over the range of transonic Mach numbers considered. Experimental data show that the mean angle of attack $\bar{\alpha}_0$ varies only by a fraction of a degree in the transonic Mach number range.

III. Results

A. Wing/Store Configurations Studied

Flutter boundary calculations have been completed for eight different F-16 wing/store configurations, and limit cycle oscillation calculations have been completed for several of the configurations as well. This latter LCO work is ongoing.

In Table 1, the store characteristics of the eight configurations are listed. Station numbers correspond to spanwise locations with stations 1 and 9 being the wing tips and station 5 the fuselage. The stores at each of these stations are listed in the table for each of the eight configurations. Missing entries in Table 1 indicate there is no store at that location. All mass properties were provided as generalized modal masses.

B. Structural Modal Convergence

First it is desirable to insure that a sufficient number of structural modes are used in the aeroelastic model. Table 2 shows the trend for flutter onset Mach number at 2000 and 10,000 ft for F-16 configuration 1 (see Table 1). As can be seen, just using the first two mode shapes provides a well-converged solution for the flutter onset

Table 1 F-16 weapons and stores configurations

No.	Sta 1	Sta 2	Sta 3	Sta 4	Sta 5	Sta 6	Sta 7	Sta 8	Sta 9
1	LAU-129	LAU-129/ AIM-9P	Air-to-ground missile A	Empty 370 gal tank	300 gal tank	Empty 370 gal tank	Air-to-ground missile A	LAU-129/ AIM-9P	LAU-129
2	LAU-129/ AIM-9L	LAU-129/ AIM-9L	Air-to-ground missile B	Half-full 370 gal tank	300 gal tank	Half-full 370 gal tank	Air-to-ground missile B	LAU-129/ AIM-9L	LAU-129/ AIM-9L
3	LAU-129	LAU-129/ AIM-120	General purpose bomb	Quarter-full 370 gal tank	300 gal tank	Quarter-full 370 gal tank	General purpose bomb	LAU-129/ AIM-120	LAU-129
4	LAU-129/ AIM-120	LAU-129	General purpose bomb	Full 370 gal tank	——	Full 370 gal tank	Air-to-ground missile B	LAU-129/ AIM-120	LAU-129
5	LAU-129/ AIM-120	LAU-129/ AIM-9P	Guided bomb	Full 370-gal tank	300 gal tank	Full 370 gal tank	Guided bomb	LAU-129/ AIM-9P	LAU-129/ AIM-120
6	LAU-129	LAU-129/ AIM-9P	Air-to-ground missile C	Half-full 370 gal tank	300 gal tank	Half-full 370 gal tank	Air-to-ground missile B	LAU-129/ AIM-9L	LAU-129/ AIM-9P
7	LAU-129	LAU-129/ AIM-9L	Cluster bomb	——	300 gal tank	——	Cluster bomb	LAU-129/ AIM-9L	LAU-129
8	LAU-129/ AIM-9P	LAU-129/ AIM-9P	Air-to-ground missile C	Full 370 gal tank	300 gal tank	Full 370 gal tank	Air-to-ground missile B	LAU-129/ AIM-9P	LAU-129

Table 2 Sensitivity of computed flutter onset Mach number to the number of structural modes used in the HB/LCO Model for 2000 and 10,000 ft, $\bar{\alpha}_0 = 1.5$ deg

	Altitude, ft	
Structural modes	2000	10,000
2	——	——
2, 4	0.9012	1.096
2, 4, 6	0.9018	1.098
2, 4, 6, 8	0.9042	1.108
2, 4, 6, 8, 10	0.9064	1.115
2, 4, 6, 8,10, and rigid roll	0.8994	1.103

Table 3 Flight test and computed LCO frequencies for various F-16 configurations at 2000 ft altitude

	LCO frequency, Hz	
Configuration	Flight test	Computation
1	8.0	8.4
2	5.6	5.4
3	7.0	7.1
4	5.4	5.3
5	4.4	4.4
8	5.5	5.5

Mach number for both altitudes. We take advantage of this in the remainder of the paper. Using only two structural modes helps to decrease the computational time required. The cost of the HB/LCO method is proportional to the number of structural modes used. Note, the generalized masses for the first two structural modes used in the present calculations are $\mathcal{M}_{2,2} = 1.576$ and $\mathcal{M}_{4,4} = 0.6723$ rather than $\mathcal{M}_{2,2} = 1.000$ and $\mathcal{M}_{4,4} = 1.000$ as employed in [1]. The units of mass are lbf $\times$ in./s^2.

C. Computed Flutter Boundaries

The computed flutter boundaries for the eight F-16 configurations are shown in Fig. 4 in terms of altitude versus Mach number based upon standard atmospheric conditions. Note the Mach number range over which flutter may occur varies substantially from one configuration to the next. In these calculations, the viscous Reynolds averaged Navier–Stokes version of the Duke University harmonic balance solver was used. Calculations for some of these configurations were also done using an Euler version of the CFD code. In general, the Euler code provides similar trends for the flutter onset boundary, but there are some quantitative differences. Also it has been found that the LCO response to be discussed subsequently is quite different with an Euler code versus a Navier–Stokes code. This is because flow separation is important for the configurations that exhibit LCO, and a Navier–Stokes model is required to describe flow separation.

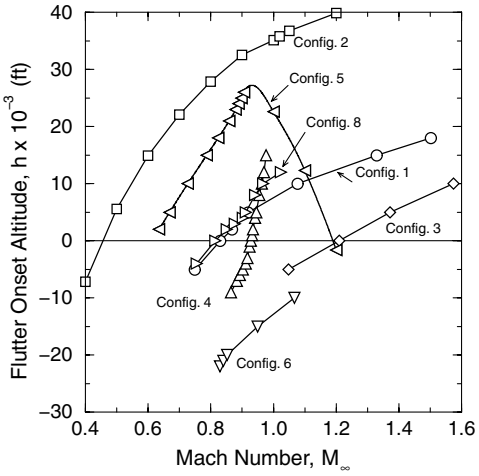

Fig. 4 Computed F-16 fighter flutter onset altitude versus Mach number.

Note that in Fig. 4 there are no results for configuration 7. This is because no flutter or LCO was found in the Mach number range shown which is in agreement with the flight-test results. Also for configuration 6, flight tests were stopped at Mach numbers less then the highest shown in Fig. 4. Again no flutter or LCO was found in the flight test in agreement with the computations. Moreover, the computed flutter boundaries shown in Fig. 4 generally agree reasonably well with the flight-test results as seen in Fig. 5. Note that a range of Mach numbers is shown for configuration 5 for flight-test results in Fig. 5. This is because flutter and LCO occur over a range of Mach numbers for configuration 5 with flutter/LCO starting at the lowest Mach number shown and ending at the highest Mach number shown. This is sometimes called a "hump" flutter/LCO mode. Also, as will be elaborated upon subsequently, the differences between computations and flight tests can be substantially attributed to uncertainties in the structural parameters such as modal frequencies.

Also it is noted that calculations using the Euler inviscid flow version of the CFD code show generally less satisfactory agreement with the flight test. However, these Euler results in turn are generally better than those obtained using a doublet-lattice aerodynamic model which of course are not applicable in the transonic Mach number range. Because the Euler fluid model failed dramatically to predict the LCO responses computed by the Navier–Stokes model and as

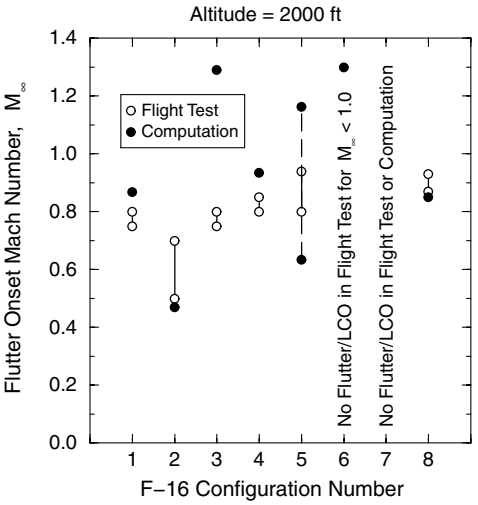

Fig. 5 Flutter Mach number characteristics for each F-16 fighter configuration.

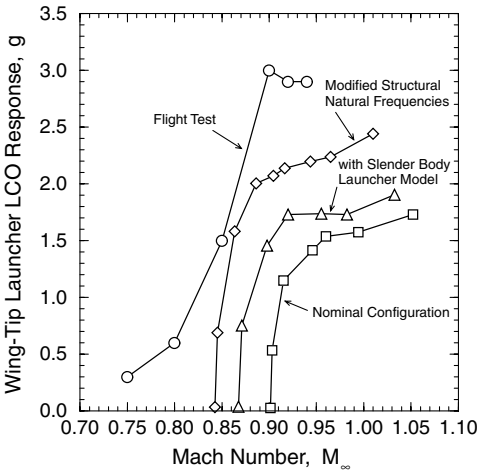

Fig. 6 F-16 configuration 1 computed and flight-test forward wing-tip launcher accelerometer LCO response level versus Mach number for an altitude of 2000 ft and a mean angle of attack of $\bar{\alpha}_0 = 1.5$ deg.

Table 4 F-16 fighter configuration natural frequencies (via NASTRAN)

Mode	Configuration 1	Configuration 2	Configuration 3
First bending (f_{1ab})	8.17 Hz	5.47 Hz	6.50 Hz
First twisting (f_{1at})	8.67 Hz	5.74 Hz	7.32 Hz
Second bending (f_{2ab})	10.9 Hz	7.87 Hz	8.37 Hz
Second twisting (f_{2at})	12.3 Hz	8.01 Hz	8.97 Hz
$f_{1at} - f_{1ab}$	0.504 Hz	0.265 Hz	0.820 Hz

observed in flight tests, only a limited number of Euler calculations were done. For those cases, the flutter Mach number predicted by the Euler model was within about 25% of that predicted by the Navier–Stokes model. The LCO amplitudes predicted by the Euler fluid model were well beyond the scale shown on the LCO response figures and much larger than those observed in either the Navier–Stokes model results or the flight tests. This difference in Euler versus Navier–Stokes results is because the nonlinear mechanism that produces LCO is flow separation combined with shock motion in the absence of structural nonlinearities. However, it is still an open question as to whether structural nonlinearities such as friction at the attachments of the stores to the wing may be important and possibly responsible for some of the remaining differences between computations and flight tests.

Table 3 shows a comparison between measured and computed frequencies at Mach numbers just beyond the onset of LCO for the several configurations where LCO was observed. The agreement is generally quite good and it is noted that the LCO frequency does not vary rapidly with Mach number.

D. Correlation of Computations and Flight Tests

In Fig. 6, a comparison of computational and flight-test results is shown for configuration 1 for both the flutter boundary and also for the LCO response. This is a plot of wing-tip acceleration response versus Mach number at a fixed altitude of 2000 ft. The flight-test results are shown by the curve with the open circles. Three different computational results are shown. The curve with the open squares shows the results for the nominal configuration with the aerodynamics of the stores neglected. The curve with the open triangles includes the effects of the aerodynamics of the wing-tip launcher using slender body aerodynamic theory. Note this curve is in better agreement with the flight-test data. Finally, the curve with open diamonds is for a case in which we have reduced the natural frequency of the first antisymmetric bending structural mode by 0.3 Hz and the natural frequency of the first antisymmetric torsion structural mode by 0.35 Hz. This results in a flutter onset frequency of $f = 8.1$ Hz and a flutter onset Mach number of $M_\infty = 0.84$; both quantities are now closer to the flight-test values. This change was deliberately selected to improve the agreement with flight-test data, that is, the computational model has been "tuned" to the experiment. As can be seen, the tuning has been successful. Of course, if a change in structural frequency in the opposite direction is made, this leads to poorer agreement between computations and flight test with the LCO response curve moving a similar amount from the nominal response but in the opposite direction. Thus, what has been shown by the tuning is that the results for this configuration are sensitive to small and plausible changes in the structural frequencies.

A final word about the correlation between computations and flight test is warranted. Note that the computations show a precise Mach number at which flutter and the onset of LCO occurs, that is, when the wing-tip acceleration is zero. This is because we have neglected the gust response of the aircraft to atmospheric turbulence as is traditional in flutter and LCO calculations. Of course in the flight test there is always some (small) response even when there is no flutter or LCO due to atmospheric turbulence. Thus it is impossible to define a precise Mach number at which flutter begins from the flight-test data shown in Fig. 6. Recall the earlier comment regarding Fig. 5. Indeed inferring a flutter Mach number from flight-test data is a difficult art and requires a greater study of the test data than simply a plot such as is shown in Fig. 6. On the other hand, for the present purpose, this is not crucial. From Fig. 6, it is clear that neither flutter nor LCO is occurring for Mach numbers less than $M_\infty = 0.8$, but flutter onset and LCO do occur for Mach numbers greater than $M_\infty = 0.85$. And thus one can compare the computed flutter Mach number with this range from the test data. For LCO per se, the major goals are predicting the maximum LCO response level and the frequency and structural modal content of the LCO. The frequency and modal content are well predicted by the computational model, and the maximum response is reasonably well predicted as well. Note, in particular, that both flight test and computations show the flutter and LCO motion is antisymmetric with respect to the roll axis of the aircraft. Also, both the computations and flight tests have shown that the dominant structural modes are the lowest antisymmetric bending and torsion modes for configuration 1 as well as for the other configurations studied here that have symmetrically placed stores.

E. Sensitivity of Flutter and Limit Cycle Oscillation to Uncertainties in Structural Natural Frequencies

In Table 4, the most important antisymmetric structural natural frequencies are shown for configurations 1–3. Note that the first two (dominant) frequencies are closest for configuration 2, and farthest apart for configuration 3, with configuration 1 in between. Because the flutter mechanism is found to be primarily a coupling between the first two structural modes in both the computations and flight tests, this suggests that small uncertainties in the structural natural frequencies would show the greatest effect on the flutter boundary for configuration 2 and the smallest effect on configuration 3. And indeed computations show this to be true (see Fig. 7).

This sensitivity to small (almost imperceptible) differences in structural natural frequencies may explain the greater variation in flight-test results for configuration 2 versus configuration 3. That is, relatively minor differences due to manufacturing or maintenance tolerances could lead to small, but significant differences in structural natural frequencies from one aircraft to the next or from one flight to the next.

Of course, one could tune the computational model by adjusting the structural frequencies so that the computed flutter boundary is in good agreement with the flight test. But that has not been done for configuration 2 or 3.

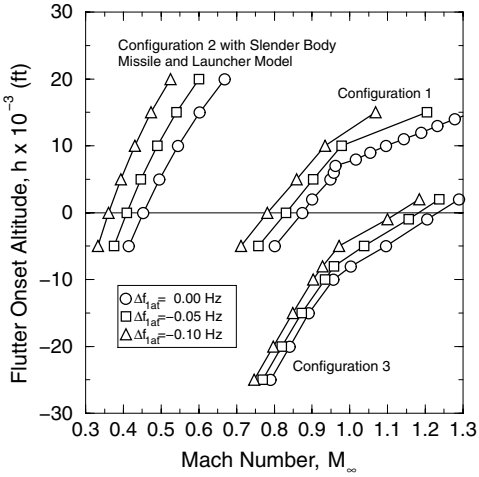

Fig. 7 Computed F-16 fighter flutter onset altitude structural frequency effect.

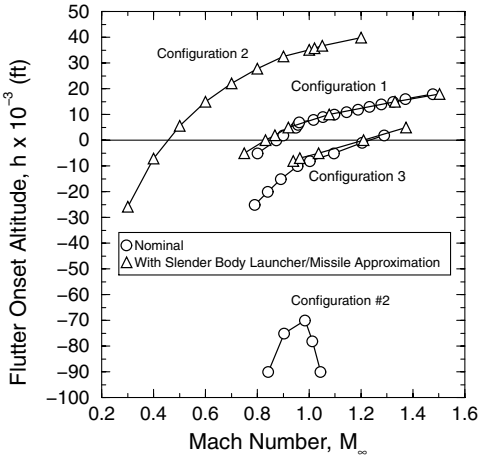

Fig. 8 The effect of slender body aerodynamic modeling for wing-tip launchers and missiles on computed F-16 fighter flutter onset altitude versus Mach number for F-16 configurations 1–3.

F. Sensitivity of Flutter and Limit Cycle Oscillation to Modeling of Aerodynamics of the Stores

All of the calculations reported above are for aerodynamics of the wing-tip launcher/missile included. In the first calculations done for the F-16 configurations, the wing-tip store aerodynamics were not included. But subsequently it has been found that they can be important for some configurations, but not for all. As an example of this, see Fig. 8. Here results are shown for configurations 1–3 with and without the aerodynamics of the wing-tip store included. The two results are virtually the same for configurations 1 and 3, but quite different for configuration 2. Why is this?

Configuration 2 has a tip missile plus launcher on each wing tip, whereas configurations 1 and 3 only have a launcher but not a missile. Computationally it is found that it is the missile and more particularly the fins of the missiles that contribute the aerodynamic forces that are important and critical for configuration 2. The results shown in Figs. 4 and 5 include the aerodynamic effects of the tip missiles.

G. Ongoing Studies

Currently we are studying configurations for which the stores on one wing are different from those on the other, so-called asymmetric configurations. The preliminary finding is that more structural modes will be required in the flutter and LCO computations and that in general the nature of the flutter and LCO is more complex and the correlation between computations and test may be less satisfactory for asymmetric configurations. However, no definitive conclusions have been reached as yet.

IV. Conclusions

Computational simulation is now capable of describing the principal features of flutter and limit cycle oscillations of modern fighter aircraft. Harmonic balance solutions are a key to such simulations. Here the emphasis has been on modeling aerodynamic nonlinearities. Future studies of possible structural nonlinearities are also needed.

A state-of-the-art CFD RANS code has been used to compute flutter onset boundaries and LCO response. The following conclusions have been reached:

1) An Euler or Navier–Stokes based CFD code is required to predict transonic flutter, and a Navier–Stokes code is required to predict LCO.

2) Good correlations have been shown between the computations and flight tests for flutter onset and LCO for the F-16 fighter, but the computational and flight-test results are sensitive to small uncertainties in structural frequencies and the aerodynamic modeling of wing-tip missile fins.

3) The correlations between the computations and flight test for the F-16 fighter are mixed for LCO amplitude prediction, though the LCO frequency and structural modal participation are usually well predicted. Possible improvements in the computational models include CFD modeling of flow separation on the missile fins and the modeling of nonlinearities in structural attachment of the missile to the wing.

References

[1] Thomas, J. P., Dowell, E. H., Hall, K. C., and Denegri, C. M., Jr., "Virtual Aeroelastic Flight Testing for the F-16 Fighter with Stores," AIAA Paper 2007-1640, 2007.

[2] Thomas, J. P., Dowell, E. H., Hall, K. C., and Denegri, C. M., Jr., "An Investigation of the Sensitivity of F-16 Fighter Limit Cycle Oscillations to Uncertainties," AIAA Paper 2006-1847, 2006.

[3] Thomas, J. P., Dowell, E. H., Hall, K. C., and Denegri, C. M., Jr., "Further Investigation of Modeling Limit Cycle Oscillation Behavior of the F-16 Fighter Using a Harmonic Balance Approach," Paper 2005-1917, 2005.

[4] Thomas, J. P., Dowell, E. H., Hall, K. C., and Denegri, C. M., Jr., "Modeling Limit Cycle Oscillation Behavior of the F-16 Fighter Using a Harmonic Balance Approach," AIAA Paper 2004-1696, 2004.

[5] Hall, K. C., Thomas, J. P., and Clark, W. S., "Computation of Unsteady Nonlinear Flows in Cascades Using a Harmonic Balance Technique," *AIAA Journal*, Vol. 40, No. 5, May 2002, pp. 879–886. doi:10.2514/2.1754

[6] Thomas, J. P., Dowell, E. H., and Hall, K. C., "Nonlinear Inviscid Aerodynamic Effects on Transonic Divergence, Flutter and Limit Cycle Oscillations," *AIAA Journal*, Vol. 40, No. 4, April 2002, pp. 638–646. doi:10.2514/2.1720

[7] Thomas, J. P., Dowell, E. H., and Hall, K. C., "Modeling Viscous Transonic Limit Cycle Oscillation Behavior Using a Harmonic Balance Approach," AIAA Paper 2002-1414, 2002.

[8] Thomas, J. P., Dowell, E. H., and Hall, K. C., "A Harmonic Balance Approach for Modeling Three-Dimensional Nonlinear Unsteady Aerodynamics and Aeroelasticity," American Society of Mechanical Engineers Paper IMECE-2002-32532, 2002.

[9] Denegri, C. M., Jr. and Dubben, J. A., "F-16 Limit Cycle Oscillation Analysis Using Transonic Small-Disturbance Theory," AIAA Paper 2005-2296, 2005.

[10] Denegri, C. M., Jr., and Dubben, J. A., "In-Flight Wing Deformation Characteristics During Limit Cycle Oscillations," AIAA Paper 2003-1426, 2003.

[11] Denegri, C. M., Jr., "Limit Cycle Oscillation Flight Test Results of a Fighter with External Stores," *Journal of Aircraft*, Vol. 37, No. 5, 2000, pp. 761–769. doi:10.2514/2.2696

[12] Parker, G. H., Maple, R. C., and Beran, P. S., "Analysis of Store Effects on Limit-Cycle Oscillation," AIAA Paper 2006-1846, 2006.

[13] Parker, G. H., and Maple, R. C., "The Role of Viscosity in Store-Induced Limit-Cycle Oscillation," AIAA Paper 2005-1916, 2005.

[14] Lieu, T., and Farhat, C., "Adaptation of Pod-Based Aeroelastic ROMs for Varying Mach Number and Angle of Attack: Application to a Complete F-16 Configuration," AIAA Paper 2005-7666, 2005.

[15] Lieu, T., Farhat, C., and Lesoinne, M., "POD-Based Aeroelastic Analysis of a Complete F-16 Configuration: ROM Adaptation and Demonstration," AIAA Paper 2005-2295, 2005.

[16] Prananta, B. B., Kok, J. C., Spekreijse, S. P., Hounjet, M. H. L.., and Meijer, J. J., "Simulation of Limit Cycle Oscillation of Fighter Aircraft at Moderate Angle of Attack," National Aerospace Laboratory NRL TR NRL-TP-2003-526, 2003.

[17] Melville, R., "Nonlinear Mechanisms of Aeroelastic Instability for the F-16," AIAA Paper 2002-0871, 2002.

[18] Ni, R.-H., "A Multiple Grid Scheme for Solving the Euler Equations," *AIAA Journal*, Vol. 20, No. 11, Nov. 1982, pp. 1565–1571. doi:10.2514/3.51220

[19] Davis, R. L., Ni, R. H., and Bowley, W. W., "Prediction of Compressible, Laminar Viscous Flows Using a Time-Marching Control Volume and Multiple-Grid Technique," *AIAA Journal*, Vol. 22, No. 11, Nov. 1984, pp. 1573–1581. doi:10.2514/3.8820

[20] Saxor, A. P., "A Numerical Analysis of 3-D Inviscid Stator/Rotor Interactions Using Non-Reflecting Boundary Conditions," Massachusetts Institute of Technology, TR 209, March 1992, Gas Turbine Laboratory.

[21] Spalart, P. R., and Allmaras, S. R., "A One Equation Turbulence Model for Aerodynamic Flows," AIAA Paper 92-0439, 1992.